
One Size Doesn't Fit All: Adaptive Label Smoothing

Ujwal Krothapalli

Department of Electrical and Computer Engineering
Virginia Tech
Blacksburg, VA 24061
ujjwal@vt.edu

A. Lynn Abbott

Department of Electrical and Computer Engineering
Virginia Tech
Blacksburg, VA 24061
abbott@vt.edu

Abstract

This paper concerns the use of objectness measures to improve the calibration performance of Convolutional Neural Networks (CNNs). Objectness is a measure of likelihood of an object from *any* class being present in a given image. CNNs have proven to be very good classifiers and generally localize objects well; however, the loss functions typically used to train classification CNNs do not penalize inability to localize an object, nor do they take into account an object's relative size in the given image. We present a novel approach to object localization that combines the ideas of objectness and label smoothing during training. Unlike previous methods, we compute a smoothing factor that is *adaptive* based on relative object size within an image. We present extensive results using ImageNet and OpenImages to demonstrate that CNNs trained using *adaptive* label smoothing are much less likely to be overconfident in their predictions, as compared to CNNs trained using hard targets. We also show qualitative results using class activation maps to illustrate the improvements.

1 Introduction

Convolutional neural networks (CNNs) have been used for addressing a variety of computer vision problems for over 2 decades [25]. In particular, CNNs have shown promising results on object detection and localization tasks since 2013 [18, 40]. Modern CNNs are overconfident in their predictions [24, 17] and they suffer from reliability issues as they are miscalibrated [14]. There is a growing demand for labeled data [29] to improve generalization performance, as increasing the number of parameters in a neural network [49, 41] will often lead to overfitting of training data, and obtaining an exponentially large labeled dataset is very expensive. Safely deploying deep learning based models has become a more immediate challenge [2], as a community, apart from obtaining high accuracies, we also need to provide reliable uncertainty measures of CNNs. By having reliable confidence measures for CNNs, we can improve precision by not acting with certainty when uncertain predictions are produced, as in the case of safety-critical systems.

Regularization is key in improving generalization and minimizing overfitting characteristics of CNNs. Recently [42] employed label smoothing, providing soft labels that are a weighted average of the hard targets and uniform distribution over classes during training to improve learning speed and generalization performance. In the case of classification CNNs, ground-truth labels are typically provided as a one-hot representation of class probabilities. These labels consist of 0s and 1s, with

a single 1 indicating the pertinent class in a given label vector. Soft targets improve the training signal by not providing hard targets to compute the cross entropy loss but a weighted average with a uniform distribution over all classes using a fixed smoothing factor [42, 31]. Label smoothing minimizes the gap between the logits of the classes and shows improvement in learning speed and generalization; in contrast, hard targets tend to increase the values of the logits and produce overconfident predictions [42, 31].

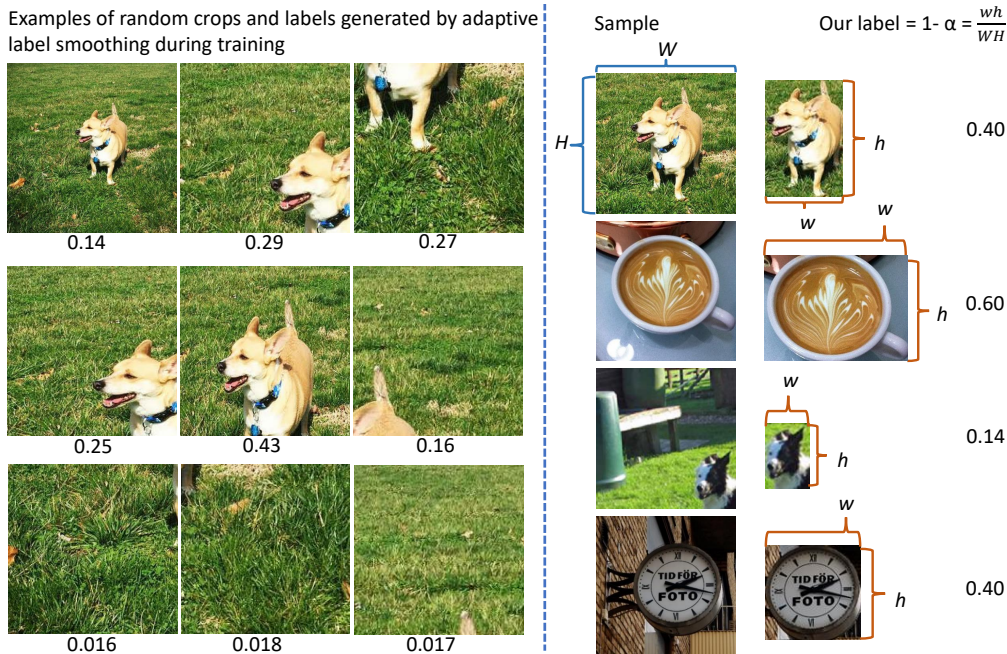


Figure 1: Random crops of images are often used when training classification CNNs to help mitigate size, position and scale bias (left half of figure). Unfortunately, some of these crops miss the object as they do not have any object location information. Traditional hard label and smooth label approaches do not account for the proportion of the object being classified and use a fixed label of ‘1’ or ‘0.9’ in the case of label smoothing. Our approach (right half) smooths the hard labels by taking into account the objectness measure to compute an *adaptive* smoothing factor. The objectness is computed using bounding box information as shown above. Our approach helps generate accurate labels during training and penalizes low-entropy (high-confidence) predictions for context-only images (the main object is completely or mostly absent).

Object detection [13] is a well-studied problem and most approaches need bounding box information during training. Recently, [10] proposed using novel synthetic images to improve the object detection performance by augmenting training data using object location information. However, classification CNNs have not exploited bounding box information to regularize CNNs on large datasets to our knowledge. Objectness was first introduced by [1], and the role of objectness has been studied extensively since then. Quantifying the likelihood an image window contains an object belonging to any class makes the measure class agnostic. Object detectors specialize in a few classes, but objectness is class agnostic by definition.

When training a classifier, cross entropy loss is employed but it does not penalize incorrect spatial attention, making CNNs often overfit to context or texture rather than the pertinent object [11], as shown in the left half of 1. The bottom row displays samples with negligible amounts of ‘Dog’ pixels and traditional methods would label them as ‘Dog’, causing CNNs to output incorrect predictions with a high confidence when presented with images of backgrounds or just context. Adaptive label smoothing (our approach) involves using bounding box information to smooth the hard labels of a classifier, as displayed to the right in figure 1. Traditional approaches [47, 43, 18, 40] use random resize and random crop augmentation, and sometimes lose the pertinent object in the training sample. Our approach adapts label smoothing by deriving the smoothing factor using the objectness

measure. When compared to approaches based on hard labels, sample mixing and label smoothing, our approach improves object detection and calibration performance.

We believe that our approach addresses significant problems that are associated with current training techniques. In particular, random cropping of images is a common augmentation technique during training of ResNet, but occasionally the crop misses the object entirely. In such a case, the equivalent of a one-hot label is typically provided, with the result that the system is steered toward increased dependence on background (context) portions of the image. We argue that one-hot representations are too limiting, and our adaptive approach to label smoothing makes it possible for the classifier to avoid overconfidence in many cases. In particular, our approach accomplishes the following: 1) Our labels not only indicate the presence of an object but also tell the classifier the gross proportion of the object in a given image. This implicit regularization guides the classifiers to avoid producing high confidence values when the object pixels are lower in proportion. On the other hand, if a random crop contains mostly object pixels, then the classifier will be encouraged to produce higher-confidence predictions. 2) A traditional classifier will tend to generate decisions with high confidence values even when images containing only background (no objects) are presented. Formally, classifiers often produce overconfident predictions. Overconfidence is particularly a problem for safety critical applications. With our approach, the system is trained to produce lower confidence predictions with out-of-distribution samples or background-only images are presented. Low confidence predictions from our approach are meaningful for rejecting false positives. High confidence approaches are hard to threshold as most predictions have high confidence even when they are wrong. 3) Traditional classifiers “cheat” by relying heavily on context. Although context helps increase computed accuracy for a given dataset, such reliance is not viable for real-world applications. During training, we assume that every class is equiprobable when only background is provided.

Our approach uses labels that are more accurate than any of the previous approaches when random cropping and scaling of images are applied during training. To our knowledge, almost all classifiers trained on ImageNet use random crop and scaling based augmentation to regularize. This ‘randomness’ forces the CNNs to rely on context rather than the pertinent object, our approach uses bounding box labels to produce labels in an adaptive way during training. To quantify context dependence, we used bounding box annotations on the 50K validation images, removed all objects and replaced the pixels with image mean. Hard label approach had an accuracy of 6.3% with an average confidence of 0.29, label smoothing predicted with an accuracy of 6.1% and an average confidence of 0.2, CutMix had an accuracy of 9.2% with an average confidence of 0.2. All these methods produced high confidence predictions on images with no objects present using pure context bias. Our approach had an accuracy of 4.7% and an average confidence of 0.02. We have an order of magnitude improvement in performance over recent baselines as our approach helps CNNs produce confidence based on the relative size of the pertinent object. The main contribution of this work is that we have developed a novel way to train classification CNNs using *adaptive* label smoothing. To demonstrate improved classification performance with less likelihood of overconfidence, we trained 20 classifiers and evaluated them on four popular datasets and show the efficacy of using object size in an implicit way.

2 Related Work

Bias exhibited by machine learning models can be attributed to many underlying statistics present in datasets and model architectures [4, 51] including context, object texture [11], size, shape and color in the case of images. Various approaches to mitigate bias have been proposed [3, 6, 11] in recent years. Our approach produces high entropy predictions when context-only images are provided as input during inference, as we aim to learn the size of the relevant object within the image and classify it, instead of relying on context to produce a prediction.

The authors of AlexNet [19] employed random cropping and horizontal flipping methods when they surpassed the performance of traditional machine learning approaches in 2012. Traditionally, any label preserving transformation on an input image is considered to help regularize a CNN. Randomly cropping a given image during training prevents overfitting the scale or location of the object; flipping an image improves the generalization to view points. The random noise class of data augmentation methods [9, 52] mask random regions of an input image with zeros. Random noise based methods may accidentally erase the pertinent object in a given image and force the CNN to rely purely on context to make a prediction, this contributes to label noise. The authors of DropBlock [12]

have used this technique (applying random noise to feature space) to obtain better generalization. Authors of AutoAugment [7] used reinforcement learning dynamically during training to learn the best combination of existing data augmentation methods.

In contrast to augmentation based approaches that manipulate the input but not the corresponding label, our approach regularizes classification CNNs by computing a label based on the proportion of the object being classified in a given random crop of the training sample. The latest work in the area of data augmentation uses samples from different classes and changes expected outputs to predict a probability distribution based on the number and intensity of pixels represented by each class. The authors of Mixup [50, 44] use alpha blending (weighted sum of pixels from two different classes), and apply blending weights to corresponding labels. The authors of CutMix and RICAP [47, 43] also use soft labels by cropping different regions and classes of images and ‘mixing’ the labels in matching proportions to corresponding regions in the final augmented sample. The sample mixing based approaches above do not rely on object size when ‘mixing’ regions in images and computing the label. Conversely, our approach uses bounding box information to apply a smoothing factor based on the object’s size relative to the image size to produce a soft label without mixing the samples.

Calibration of CNNs is important as predictions need to be equally accurate and confident. Calibration and uncertainty estimation of predictors has been an ongoing interest to the machine learning community [33, 8, 37, 26, 48]. Bayesian binning into quantiles (BBQ) [34] was proposed for binary classification and beta calibration [20] employed logistic calibration for binary classifiers. In the context of CNNs, [15] proposed a temperature scaling approach to improve calibration performance of pre-trained models. Calibration has been explored in multiple directions; popular approaches to calibrate CNNs are to transform outputs of pre-trained models using approximate bayesian inference [28], or to use a special loss function to help regularize the model [36, 22] during training. Our approach is loosely related to the latter class of methods. Our work also relates to label smoothing proposed first by [42], with its applicability for many tasks explored by [36]; [46] applies dropout-like noise to the labels. Recently, [31] explored the benefits of label smoothing; apart from having a regularizing effect, label smoothing helps reduce intra-class distance between samples [31]. Another approach to calibrate CNNs was proposed by [30], using a special loss function and temperature scaling, the authors were able to obtain state-of-the-art calibration performance. Label smoothing also improves calibration performance of CNNs [30].

Contrasting previously discussed methods, our approach involves using hard labels multiplied by the objectness measure and obtaining a uniform distribution over all other classes when input images are devoid of pertinent objects. We do not change our loss function as opposed to [30]. Our approach can be described as a variant of label smoothing, employing an *adaptive* label smoothing approach that is unique to every training sample as it accounts for object size. To our knowledge, we are the first to apply *adaptive* label smoothing to train image classification CNNs.

The objectness is computed using bounding box information during training. CNNs trained using hard labels produce ‘peaky’ probability distributions without considering the spatial size of the pertaining object. Our approach produces outputs that are softer and the peaks correspond to the spatial footprint of the object being classified as shown in figure 2.

3 Method

Consider $D = \langle (\mathbf{x}_i, y_i) \rangle_{i=1}^N$ to be a dataset consisting of N independent and identically distributed real-world images belonging to K different classes. Let \mathcal{X} represent the set of images, and let \mathcal{Y} denote the set of ground-truth class labels. Sample i consists of the image $\mathbf{x}_i \in \mathcal{X}$ along with its corresponding label $y_i \in \mathcal{Y} = \{1, 2, \dots, K\}$. Let f_θ represent the CNN classifier with model parameters θ . The predicted class is $\hat{y}_i = \operatorname{argmax}_{y \in \mathcal{Y}} \hat{p}_{i,y}$, where $\hat{p}_{i,y} = f_\theta(y|\mathbf{x}_i)$ is the computed probability that image \mathbf{x}_i belongs to class y .

Let z_i represent the one-hot encoding of label y_i . Following [42], the hard label z_i can be converted to soft label \tilde{z}_i using $\tilde{z}_i = z_i(1 - \alpha) + (1 - z_i)\alpha/(K - 1)$, where $\alpha \in [0, 1]$ is a fixed hyperparameter. This is the standard procedure known as label smoothing.

A novelty of our approach is to make α *adaptive*, calculating the value based on the relative size of an object within a given training image. Using the bounding box annotations available for the images in the dataset, we generate object masks. We apply the same augmentation transform (scale,

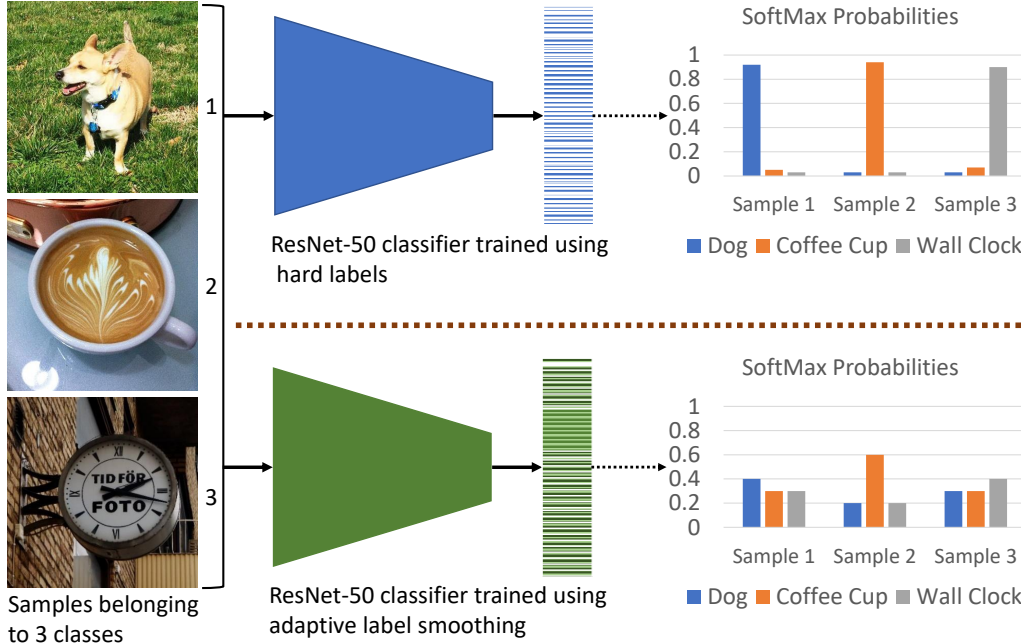


Figure 2: Hard-label and label-smoothing based approaches (top half of the figure) do not take into account the proportion of the object being classified. Our approach (bottom half) weights soft labels using the objectness measure to compute an *adaptive* smoothing factor.

crop) to the masks and compute the objectness score on the fly for every training image. Let the image width and height be denoted by (W, H) and the object width and height be denoted by (w, h) . The ratio α is computed as $\alpha = 1 - \frac{wh}{WH}$. The soft label \tilde{z}_i is computed as before. We also explore a weighted combination of *adaptive* label smoothing and hard labels. To do this, we introduce parameter $\beta \in [0, 1]$ to determine degree of *adaptive* label smoothing being applied. The setting $\beta = 0$ corresponds to the case of classic hard labels. The soft label in this case is computed as $\tilde{z}_i = (z_i(1 - \alpha) + (1 - z_i)\alpha / (K - 1))\beta + (1 - \beta)z_i$.

4 Experiments

In this section, we provide a description of the datasets used in our experiments, introduce some of the commonly used metrics for calibration of CNNs and describe our implementation details. We then discuss the merits of our approach and answer important questions related to applicability to transfer learning in an object detection setting, and we discuss the effect of using different types of labels during training in an ablative manner. We use ResNet-50 [16] for all our experiments.

4.1 Datasets

As indicated in table 1, we have used different training datasets that are based on ImageNet-1K dataset [40]. ImageNet-1K consists of 1.2M training images and 50K validation images spanning 1K categories. As only 38% of ImageNet training images have bounding-box annotations, we distinguish these experiments from those trained on the full dataset. We use standard data-augmentation strategies for all methods and train all our models for 300 epochs starting with a learning rate of 0.1 and decayed by 0.1 at epochs 75, 150, and 225 using a batch size of 256.

The first 6 rows of the table employ the standard dataset for training. However, as our method needs object proportions, we use a subset of the standard ImageNet dataset that have bounding boxes (0.474M). These results are shown in the next 8 rows of table 1. To generate the ‘mask’ version, we make sure that only one object is present in a given image and ‘mask’ all other objects replacing them with pixel means. We use this version of the dataset derived from the 0.474M subset and identify the approach with ‘(mask)’ next to the method in table 1. We end up with about 54K more

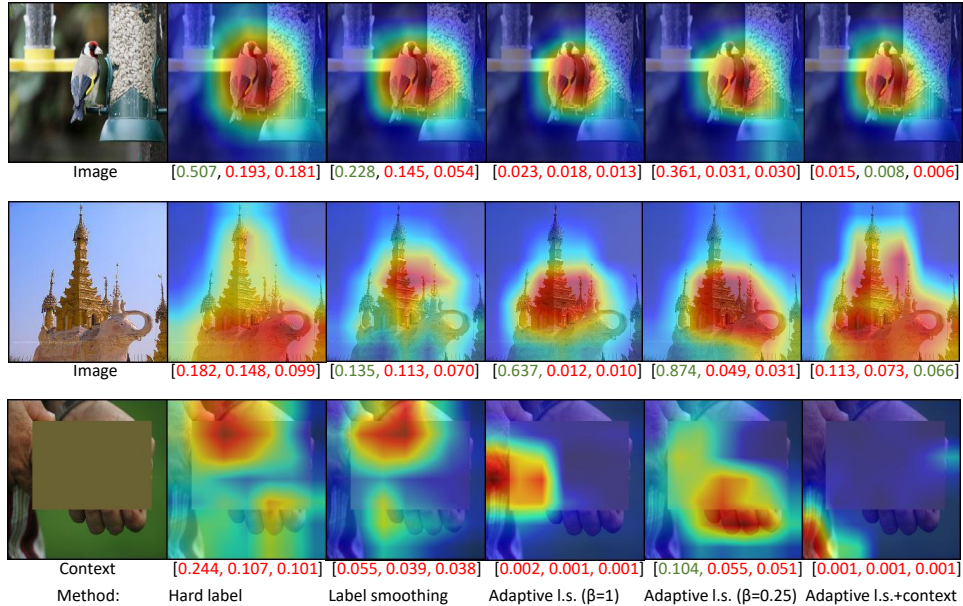


Figure 3: Examples of class activation maps (CAMs). These were obtained using the implementation of [5]. Two columns on the left show results for baseline CNNs using hard labels and standard label smoothing. Our approach, *adaptive* label smoothing (“adaptive l.s.”), is illustrated in the three columns on the right. Our technique produces high-entropy predictions and shows an improved localization performance. The values under each CAM represent the top three probabilities, with green indicating the pertinent class and red indicating an incorrect prediction.

images as some ImageNet images have multiple annotated objects. Lastly, we generate another dataset that is devoid of any object altogether. We sample about 15% of the time from this dataset during training of one of our approaches, and the label generated for these methods is a vector of uniform probability distribution across 1000 classes. The idea is that when no objects are present in a sample, a CNN should produce a high-entropy prediction. For validation, we use the validation set of [40] (V1) and the newly released ImageNetV2 set [38]. Specifically, we use the more challenging ‘MatchedFrequency’ set of images. The different validation sets are identified in the ‘Val.’ column of table 1.

We also used a portion of the OpenImages [23] dataset. More specifically, we used the object-detection version of the dataset, consisting of 600 classes and 1.7M images with bounding boxes. We selected a subset of these images and trained 5 classifiers. (For information on how we subsampled this dataset, please see the supplementary section.) For a fair comparison with our ImageNet-based models, we matched the number of iterations and reduced the total epochs. We trained all our OpenImages models for 72 epochs starting with a learning rate of 0.1, and decayed by 0.1 at epochs 18, 36, and 54 using a batch size of 256. To measure the transfer-learning ability of the representations learned by our classifiers, we used the challenging [27] dataset to obtain the results described in-2. The dataset consists of about 230K training images and we use the ‘minimal’ validation set of 5K images.

4.2 Classification and calibration

This section identifies various calibration metrics used by the community and discusses our results obtained on the popular [40, 38] datasets. We use the implementation of [45] on all of our classifiers to generate the results in table 1. To evaluate the performance of *adaptive* label smoothing we use five metrics that are very common: *accuracy*, *expected calibration error* (ECE) [34], *maximum calibration error* (MCE) [34], *overconfidence* [32], and *underconfidence* [32]. We computed ECE using 100 bins and 15 bins. The authors of [45, 21] discuss the advantages of using 100 bins in greater detail.

Table 1: Classification and calibration results with ImageNet. For a detailed explanation of the metrics please refer to 4.2. ‘O.conf’ and ‘U.conf’ refer to overconfidence and underconfidence scores.

Method	Val. Set	Train N	ACC	ECE 100	ECE 15	MCE	O.conf	U.conf
Hard Label	V1	1.28M	0.769	0.062	0.045	0.284	0.582	0.100
Hard Label	V2	1.28M	0.647	0.131	0.099	0.664	0.538	0.131
CutMix	V1	1.28M	0.788	0.035	0.022	0.267	0.520	0.162
CutMix	V2	1.28M	0.661	0.094	0.051	0.817	0.485	0.192
RICAP	V1	1.28M	0.782	0.032	0.021	0.284	0.553	0.131
RICAP	V2	1.28M	0.663	0.108	0.072	0.697	0.516	0.165
Hard Label	V1	0.474M	0.669	0.104	0.093	0.347	0.558	0.123
Hard Label	V2	0.474M	0.543	0.171	0.148	0.759	0.520	0.154
CutMix	V1	0.474M	0.689	0.032	0.017	0.167	0.456	0.209
CutMix	V2	0.474M	0.577	0.100	0.050	0.517	0.421	0.248
Label Smoothing	V1	0.474M	0.691	0.055	0.051	0.354	0.401	0.248
Label Smoothing	V2	0.474M	0.558	0.102	0.047	0.512	0.368	0.283
A. L. S. (Ours)	V1	0.474M	0.655	0.191	0.186	0.461	0.255	0.401
A. L. S. (Ours)	V2	0.474M	0.532	0.185	0.158	0.661	0.217	0.441
Hard Label (mask)	V1	0.528M	0.680	0.088	0.076	0.259	0.549	0.132
Hard Label (mask)	V2	0.528M	0.559	0.155	0.127	0.686	0.507	0.163
CutMix (mask)	V1	0.528M	0.698	0.032	0.020	0.249	0.477	0.197
CutMix (mask)	V2	0.528M	0.576	0.110	0.067	0.614	0.449	0.228
Label Smoothing (mask)	V1	0.528M	0.687	0.051	0.046	0.430	0.407	0.244
Label Smoothing (mask)	V2	0.528M	0.563	0.108	0.048	0.524	0.374	0.281
A. L. S. (mask)	V1	0.528M	0.648	0.186	0.182	0.463	0.246	0.396
A. L. S. (mask)	V2	0.528M	0.528	0.185	0.160	0.687	0.209	0.441
A. L. S. (mask) (Beta=0.75)	V1	0.528M	0.681	0.146	0.142	0.377	0.319	0.337
A. L. S. (mask) (Beta=0.75)	V2	0.528M	0.556	0.146	0.113	0.572	0.274	0.375
A. L. S. (mask) (Beta=0.25)	V1	0.528M	0.684	0.059	0.052	0.244	0.402	0.244
A. L. S. (mask) (Beta=0.25)	V2	0.528M	0.561	0.109	0.059	0.627	0.369	0.285
A. L. S.+Context (mask)	V1	0.528M	0.637	0.174	0.169	0.431	0.251	0.390
A. L. S.+Context (mask)	V2	0.528M	0.515	0.177	0.147	0.682	0.221	0.437
A. L. S.+CutMix (mask)	V1	0.528M	0.442	0.349	0.332	0.559	0.047	0.843
A. L. S.+CutMix (mask)	V2	0.528M	0.346	0.292	0.265	0.902	0.049	0.851

ECE is defined as the expected absolute difference between a classifier’s confidence and its accuracy using a finite number of bins [34]. MCE is defined as the maximum absolute difference between a classifier’s confidence and its accuracy of each bin [34]. Overconfidence is the average confidence of a classifier’s false predictions and underconfidence as the average uncertainty on its correct predictions [45, 32].

The results in table 1 indicate our approaches based on *adaptive* label smoothing using the abbreviation ‘A. L. S.’ In general, these results have a low overconfidence score, which is highly desirable. These results demonstrate that adaptive label smoothing based CNNs seldom produce high confidence scores when they make incorrect predictions. In fact, our models are underconfident as they pay attention to the spatial footprint of the pertinent object. It is important to note that our methods outperform all baselines for the overconfidence metric.

4.3 Transfer learning for object detection

We adopt the architecture of Faster RCNN [39] adapted to use the ResNet-50 backbone. Specifically, we train all of our classifiers using the implementation of <https://github.com/jwyang/faster-rcnn.pytorch>. We train all ImageNet pre-trained models with a batch size of 16 and initial learning rate of 0.01 decayed after every 4 epochs for a total of 10 epochs. We train all OpenImages pre-trained models with a batch size of 16 and initial learning rate of 0.0075 decayed after every 4 epochs for a

Table 2: Fine-tuning on COCO using FRCNN for object detection. For a detailed explanation of the results please refer to 4.3. AP refers to average precision and AR refers to average recall at the specified Intersection over union (IoU) level.

Method	Pre-trained on	Pre-train N	AP (0.5:0.95)	AP (0.5)	AP (0.75)	AR (0.5:0.95)
Hard Label	ImageNet	1.28M	0.323	0.519	0.345	0.438
CutMix	ImageNet	1.28M	0.329	0.528	0.353	0.445
RICAP	ImageNet	1.28M	0.331	0.528	0.354	0.447
Hard Label	ImageNet	0.474M	0.290	0.479	0.309	0.415
A. L. S. (Ours)	ImageNet	0.474M	0.311	0.501	0.332	0.429
Hard Label (mask)	ImageNet	0.528M	0.290	0.482	0.307	0.415
CutMix (mask)	ImageNet	0.528M	0.312	0.509	0.329	0.428
Label Smoothing (mask)	ImageNet	0.528M	0.304	0.500	0.324	0.424
A. L. S. (mask)	ImageNet	0.528M	0.311	0.501	0.333	0.428
A. L. S. (mask) (Beta=0.75)	ImageNet	0.528M	0.309	0.498	0.331	0.427
A. L. S. (mask) (Beta=0.25)	ImageNet	0.528M	0.298	0.492	0.315	0.419
A. L. S. + Context (mask)	ImageNet	0.528M	0.303	0.490	0.323	0.421
A. L. S. + CutMix (mask)	ImageNet	0.528M	0.273	0.449	0.289	0.403
Hard Label (mask)	OpenImages	1.20M	0.295	0.484	0.313	0.416
Label Smoothing (mask)	OpenImages	1.20M	0.301	0.493	0.320	0.420
A. L. S. (mask)	OpenImages	1.20M	0.243	0.415	0.250	0.371
A. L. S. + Context (mask)	OpenImages	1.20M	0.289	0.471	0.308	0.408
A. L. S. (mask) (Beta=0.25)	OpenImages	1.20M	0.304	0.494	0.324	0.422

total of 10 epochs. We employ the standard metrics for average precision (AP) and average recall [27] at different intersection over union (IoU) levels. As shown in 2, our approach outperforms hard label and label smoothing based approaches on this downstream task. The better localization performance is also shown without fine-tuning using class activation maps in figure 3. Specifically, our approach performs almost as well as CutMix [47] using AP measures.

4.4 Ablation studies

We compare our approach with standard baselines and provide results in an ablative manner to understand the benefits and limitations of applying *adaptive* label smoothing to classification and transfer learning for object detection tasks. As shown in figure 4, increasing the value of β helps reduce model overconfidence and produces predictions that are less ‘peaky’ compared to label smoothing and hard label settings. Another interesting trend can be observed by changing the value of the β hyperparameter. As β decreases in value, the overconfidence rate goes up along with it. Average confidence of a model describes the mean confidence of a model. As our model predictions are grounded in the spatial size of the object, our average confidence values on ‘V1’ and ‘V2’ are 0.48 and 0.39, respectively; in the case of hard labels the values are 0.77 and 0.69, respectively.

In case of transfer learning, we observe that decreasing β causes the object localization performance to drop. Using implicit object size information helps CNNs localize and detect objects for downstream tasks as well.

5 Conclusion

This paper has addressed the problems of contextual bias and calibration using a novel approach called *adaptive* label smoothing. We show that bounding box information pertaining to objects can be used to compute a smoothing factor *adaptively* during training to improve the localization and calibration performance of CNNs. We use bounding box information for a portion of ImageNet [40] and OpenImages datasets to train 20 different classifiers. We show that our approach can be combined with

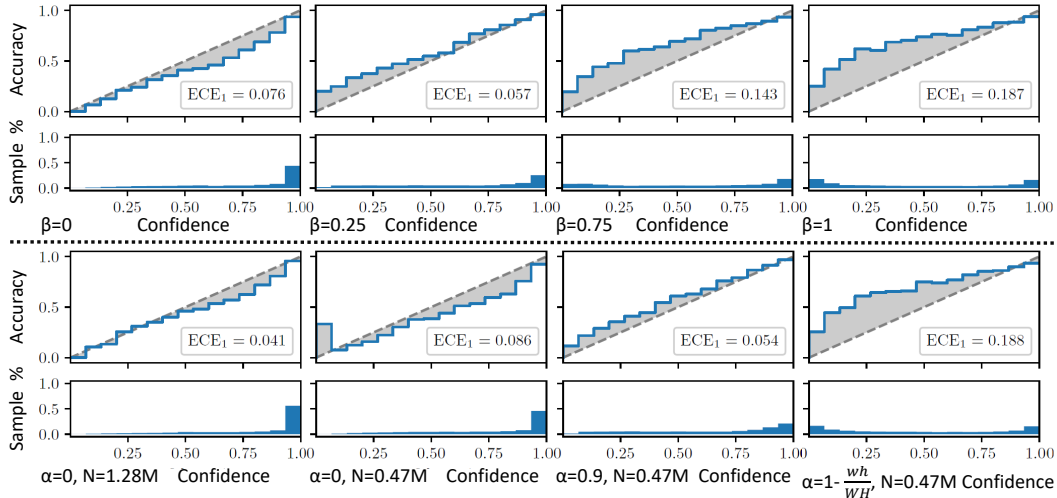


Figure 4: Reliability diagrams help understand the calibration performance [8, 35] of classifiers. We compute ECE_1 using the implementation of [45] on the validation set of ImageNet. The deviation from the dashed line (shown in gray), weighted by the histogram of confidence values, is equal to Expected Calibration Error [45]. The top half of the figure shows classifiers trained using the same dataset ($N=0.528M$), but with different values of β . The leftmost reliability diagram is the classic hard label setting and the rightmost reliability diagram is the *adaptive* label setting. The bottom half of the figure compares classifiers trained on the complete ImageNet (leftmost) with 3 classifiers trained on the subset of ImageNet with bounding box labels using different values of the α hyperparameter.

traditional label smoothing approaches to train CNNs that are calibrated and have better localization performance on the challenging MS-COCO [27] dataset after fine-tuning, compared to approaches that use hard labels or traditional label smoothing approaches. Our labels capture the object proportion in an implicit manner during training, a significantly more challenging task when compared to training with hard labels. Although our methods do not improve upon the accuracy of traditional label smoothing for the classification task, we show better regularization and calibration performance on the newly released ImageNetV2 [38] dataset. Our approach can be used to produce high entropy predictions when context-only images are provided as input.

Broader Impact

We introduce *adaptive* label smoothing with the notion that safety-critical applications need CNNs that are trained not to be overconfident in their predictions. Our intention is for decision making systems (steering inputs to an autonomous vehicle for example) to not make decisions in a definite way when the models are not confident in their predictions.

References

- [1] Bogdan Alexe, Thomas Deselaers, and Vittorio Ferrari. Measuring the objectness of image windows. *IEEE transactions on pattern analysis and machine intelligence*, 2012.
- [2] Dario Amodei, Chris Olah, Jacob Steinhardt, Paul F. Christiano, John Schulman, and Dan Mané. Concrete problems in AI safety. *arXiv preprint arXiv:1606.06565*, 2016.
- [3] Lisa Anne Hendricks, Kaylee Burns, Kate Saenko, Trevor Darrell, and Anna Rohrbach. Women also snowboard: Overcoming bias in captioning models. In *Proceedings of the European Conference on Computer Vision (ECCV)*, pages 771–787, 2018.
- [4] Peter W Battaglia, Jessica B Hamrick, Victor Bapst, Alvaro Sanchez-Gonzalez, Vinicius Zambaldi, Mateusz Malinowski, Andrea Tacchetti, David Raposo, Adam Santoro, Ryan Faulkner, et al. Relational inductive biases, deep learning, and graph networks. *arXiv preprint arXiv:1806.01261*, 2018.
- [5] Aditya Chattopadhyay, Anirban Sarkar, Prantik Howlader, and Vineeth N Balasubramanian. Grad-cam++: Generalized gradient-based visual explanations for deep convolutional networks. In *2018 IEEE Winter Conference on Applications of Computer Vision (WACV)*, pages 839–847. IEEE, 2018.

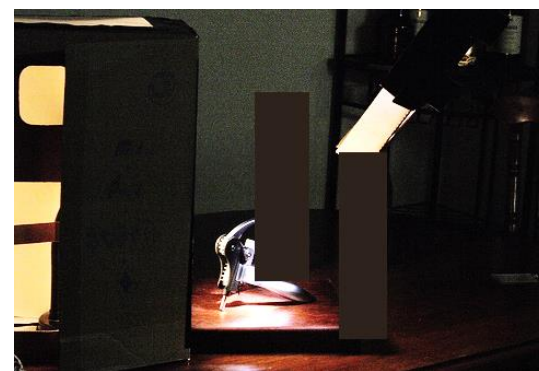
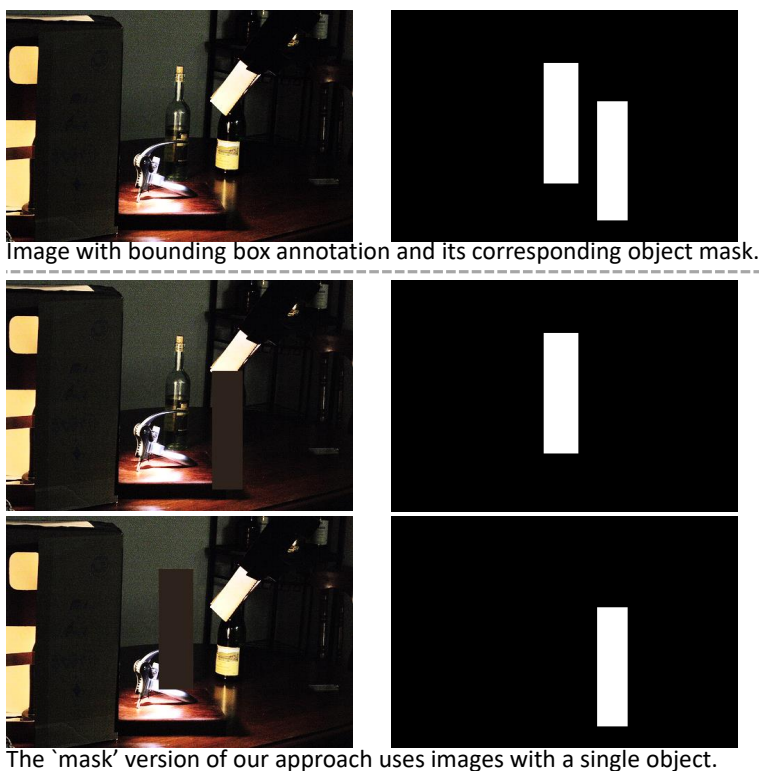
- [6] Jinwoo Choi, Chen Gao, Joseph CE Messou, and Jia-Bin Huang. Why can't it dance in the mall? learning to mitigate scene bias in action recognition. In *Advances in Neural Information Processing Systems*, pages 851–863, 2019.
- [7] Ekin D Cubuk, Barret Zoph, Dandelion Mane, Vijay Vasudevan, and Quoc V Le. Autoaugment: Learning augmentation policies from data. In *CVPR*, 2019.
- [8] Morris H. DeGroot and Stephen E. Fienberg. The comparison and evaluation of forecasters. *Journal of the Royal Statistical Society. Series D (The Statistician)*, 32:12–22, 1983.
- [9] Terrance DeVries and Graham W Taylor. Improved regularization of convolutional neural networks with cutout. *arXiv preprint arXiv:1708.04552*, 2017.
- [10] Nikita Dvornik, Julien Mairal, and Cordelia Schmid. Modeling visual context is key to augmenting object detection datasets. In *Proceedings of the European Conference on Computer Vision (ECCV)*, pages 364–380, 2018.
- [11] Robert Geirhos, Patricia Rubisch, Claudio Michaelis, Matthias Bethge, Felix A Wichmann, and Wieland Brendel. Imagenet-trained cnns are biased towards texture; increasing shape bias improves accuracy and robustness. In *ICLR*, 2019.
- [12] Golnaz Ghiasi, Tsung-Yi Lin, and Quoc V Le. Dropblock: A regularization method for convolutional networks. In *Advances in Neural Information Processing Systems*, pages 10750–10760, 2018.
- [13] Ross Girshick, Ilija Radosavovic, Georgia Gkioxari, Piotr Dollár, and Kaiming He. Detectron. <https://github.com/facebookresearch/detectron>, 2018.
- [14] Chuan Guo, Geoff Pleiss, Yu Sun, and Kilian Q Weinberger. On calibration of modern neural networks. In *Proceedings of the 34th International Conference on Machine Learning (ICML)*, 2017.
- [15] Chuan Guo, Geoff Pleiss, Yu Sun, and Kilian Q Weinberger. On calibration of modern neural networks. In *Proceedings of the 34th International Conference on Machine Learning-Volume 70*, pages 1321–1330. JMLR. org, 2017.
- [16] Kaiming He, Xiangyu Zhang, Shaoqing Ren, and Jian Sun. Deep residual learning for image recognition. In *CVPR*, 2016.
- [17] Matthias Hein, Maksym Andriushchenko, and Julian Bitterwolf. Why relu networks yield high-confidence predictions far away from the training data and how to mitigate the problem. In *Proceedings of the IEEE Conference on Computer Vision and Pattern Recognition (CVPR)*, June 2019.
- [18] Alex Krizhevsky, Ilya Sutskever, and Geoffrey E Hinton. Imagenet classification with deep convolutional neural networks. In *NIPS*, 2012.
- [19] Alex Krizhevsky, Ilya Sutskever, and Geoffrey E Hinton. Imagenet classification with deep convolutional neural networks. In *NIPS*, 2012.
- [20] Meelis Kull, Telmo Silva Filho, and Peter Flach. Beta calibration: a well-founded and easily implemented improvement on logistic calibration for binary classifiers. In *Proceedings of the 20th International Conference on Artificial Intelligence and Statistics (AISTATS)*, volume 54, pages 623–631, 2017.
- [21] Ananya Kumar, Percy Liang, and Tengyu Ma. Variance reduced uncertainty calibration. In *Advances in Neural Information Processing Systems (NeurIPS)*, 2019.
- [22] Aviral Kumar, Sunita Sarawagi, and Ujjwal Jain. Trainable calibration measures for neural networks from kernel mean embeddings. In *Proceedings of the 35th International Conference on Machine Learning (ICML)*, pages 2810–2819, 2018.
- [23] Alina Kuznetsova, Hassan Rom, Neil Alldrin, Jasper Uijlings, Ivan Krasin, Jordi Pont-Tuset, Shahab Kamali, Stefan Popov, Matteo Mallocci, Alexander Kolesnikov, et al. The open images dataset v4. *International Journal of Computer Vision*, pages 1–26, 2020.
- [24] Balaji Lakshminarayanan, Alexander Pritzel, and Charles Blundell. Simple and scalable predictive uncertainty estimation using deep ensembles. In *Advances in Neural Information Processing Systems (NeurIPS)*, pages 6402–6413, 2017.
- [25] Yann LeCun. The mnist database of handwritten digits. <http://yann.lecun.com/exdb/mnist/>, 1998.
- [26] Hsuan-Tien Lin, Chih-Jen Lin, and Ruby C Weng. A note on platt's probabilistic outputs for support vector machines. *Machine learning*, 68(3):267–276, 2007.
- [27] Tsung-Yi Lin, Michael Maire, Serge Belongie, James Hays, Pietro Perona, Deva Ramanan, Piotr Dollár, and C Lawrence Zitnick. Microsoft coco: Common objects in context. In *European conference on computer vision*, pages 740–755. Springer, 2014.
- [28] Wesley Maddox, Timur Garipov, Pavel Izmailov, Dmitry Vetrov, and Andrew Gordon Wilson. A simple baseline for bayesian uncertainty in deep learning. *arXiv preprint arXiv:1902.02476*, 2019.
- [29] Dhruv Mahajan, Ross Girshick, Vignesh Ramanathan, Kaiming He, Manohar Paluri, Yixuan Li, Ashwin Bharambe, and Laurens van der Maaten. Exploring the limits of weakly supervised pretraining. In *Proceedings of the European Conference on Computer Vision (ECCV)*, pages 181–196, 2018.
- [30] Jishnu Mukhoti, Viveka Kulharia, Amartya Sanyal, Stuart Golodetz, Philip HS Torr, and Puneet K Dokania. Calibrating deep neural networks using focal loss. *arXiv preprint arXiv:2002.09437*, 2020.
- [31] Rafael Müller, Simon Kornblith, and Geoffrey E Hinton. When does label smoothing help? In *Advances in Neural Information Processing Systems*, pages 4696–4705, 2019.

- [32] D. Mund, R. Triebel, and D. Cremers. Active online confidence boosting for efficient object classification. In *Proceedings of the IEEE International Conference on Robotics and Automation (ICRA)*, pages 1367–1373, 2015.
- [33] Allan H. Murphy. A new vector partition of the probability score. *Journal of Applied Meteorology*, 12(4):595–600, 1973.
- [34] Mahdi Pakdaman Naeini, Gregory F. Cooper, and Milos Hauskrecht. Obtaining well calibrated probabilities using bayesian binning. In Blai Bonet and Sven Koenig, editors, *Proceedings of the Conference on Artificial Intelligence (AAAI)*, pages 2901–2907, 2015.
- [35] Alexandru Niculescu-Mizil and Rich Caruana. Predicting good probabilities with supervised learning. In *Proceedings of the 22nd International Conference on Machine Learning (ICML)*, pages 625–632, 2005.
- [36] Gabriel Pereyra, George Tucker, Jan Chorowski, Łukasz Kaiser, and Geoffrey Hinton. Regularizing neural networks by penalizing confident output distributions. *arXiv preprint arXiv:1701.06548*, 2017.
- [37] John C. Platt. Probabilistic outputs for support vector machines and comparisons to regularized likelihood methods. In *Advances in Large-Margin Classifiers*, pages 61–74. MIT Press, 1999.
- [38] Benjamin Recht, Rebecca Roelofs, Ludwig Schmidt, and Vaishaal Shankar. Do imagenet classifiers generalize to imagenet? In *International Conference on Machine Learning*, pages 5389–5400, 2019.
- [39] Shaoqing Ren, Kaiming He, Ross Girshick, and Jian Sun. Faster r-cnn: Towards real-time object detection with region proposal networks. In *NIPS*, 2015.
- [40] Olga Russakovsky, Jia Deng, Hao Su, Jonathan Krause, Sanjeev Satheesh, Sean Ma, Zhiheng Huang, Andrej Karpathy, Aditya Khosla, Michael Bernstein, Alexander C. Berg, and Li Fei-Fei. Imagenet large scale visual recognition challenge. *International Journal of Computer Vision*, 115(3):211–252, 2015.
- [41] Rupesh K Srivastava, Klaus Greff, and Jürgen Schmidhuber. Training very deep networks. In *NIPS*, 2015.
- [42] Christian Szegedy, Vincent Vanhoucke, Sergey Ioffe, Jon Shlens, and Zbigniew Wojna. Rethinking the inception architecture for computer vision. In *CVPR*, 2016.
- [43] Ryo Takahashi, Takashi Matsubara, and Kuniaki Uehara. Ricap: Random image cropping and patching data augmentation for deep cnns. In *Asian Conference on Machine Learning*, pages 786–798, 2018.
- [44] Yuji Tokozume, Yoshitaka Ushiku, and Tatsuya Harada. Between-class learning for image classification. In *Proceedings of the IEEE Conference on Computer Vision and Pattern Recognition*, pages 5486–5494, 2018.
- [45] Jonathan Wenger, Hedvig Kjellström, and Rudolph Triebel. Non-parametric calibration for classification. In *Proceedings of the 23rd International Conference on Artificial Intelligence and Statistics (AISTATS)*, Proceedings of Machine Learning Research, 2020.
- [46] Lingxi Xie, Jingdong Wang, Zhen Wei, Meng Wang, and Qi Tian. Disturblabel: Regularizing cnn on the loss layer. In *Proceedings of the IEEE Conference on Computer Vision and Pattern Recognition*, pages 4753–4762, 2016.
- [47] Sangdoon Yun, Dongyoon Han, Seong Joon Oh, Sanghyuk Chun, Junsuk Choe, and Youngjoon Yoo. Cutmix: Regularization strategy to train strong classifiers with localizable features. In *ICCV*, 2019.
- [48] Bianca Zadrozny and Charles Elkan. Transforming classifier scores into accurate multiclass probability estimates. In *Proceedings of the 8th ACM International Conference on Knowledge Discovery and Data Mining (SIGKDD)*, pages 694–699, 2002.
- [49] Sergey Zagoruyko and Nikos Komodakis. Wide residual networks. *Proceedings of the British Machine Vision Conference (BMVC)*, 2016.
- [50] Hongyi Zhang, Moustapha Cisse, Yann N Dauphin, and David Lopez-Paz. mixup: Beyond empirical risk minimization. *arXiv preprint arXiv:1710.09412*, 2017.
- [51] Quanshi Zhang, Wenguan Wang, and Song-Chun Zhu. Examining cnn representations with respect to dataset bias. In *Thirty-Second AAAI Conference on Artificial Intelligence*, 2018.
- [52] Zhun Zhong, Liang Zheng, Guoliang Kang, Shaozi Li, and Yi Yang. Random erasing data augmentation. *arXiv preprint arXiv:1708.04896*, 2017.

Supplementary

1 Experimental setup

1.1 Datasets and splits



The 'context' version of our approach uses images with all the objects masked out about 15% of the time during training. The label vector for such images (context only) is a vector of uniform distribution.

Figure 1: The first row of images in the left half of the figure are an example of the ImageNet dataset ($N=0.474M$) that have bounding box annotations. We match the images from the training set of ImageNet-1K dataset with the corresponding '.xml' files included in the ImageNet object detection dataset. We then create object masks for each of the images. When applying any scaling and cropping operation to training samples, we apply the same transformation to the corresponding object masks as well. By counting the number of white pixels, we can determine the object proportion post transformation. We describe the two other approaches in the figure, the 'mask' version of our approach has a single object (for images with multiple bounding box annotations) and this version has 0.528M samples. Our approach helps generate accurate labels during training and penalizes low-entropy (high-confidence) predictions for context-only images like the example on the right half of the figure.

Our approach to create the different versions of ImageNet [6] to train our models are described in figure 1. We use the pixel means to mask all but one or all the objects using the same methodology

n09428293 241052415626070318753599468741387452165419107344749246424864317972033077187250443954008694219775353134718712368037720878368776864466576797
n04467666 312240456412042236016324228063476998355406743720827820222644437802076157456084118524373333369062974094686324952620527881364771847742329988
n04133789 12377641299137704319794287297642584169720903385031429470724835323999516298891214974098093340002415951003693145001945248024887706
n00108184 123217412282355107760858602027200879124029329516248768802382977209898320129201436629138484734042312774857932074536671279241293127672812
n00288779 12011371932054104840865117882424300477903894141926791161497783090919982073040420920044338389487583052921007843454537850146393928143950
n01856672 10411361266451043993812788214598742182208686832108680840404208848083496856525000241224808507219041091882743748433892929707421010833987
n03302122 104311120199420335004465371226697137647308943463447835910092114737142632483300027492144395553016800114166776707690637239641881833818
n02113494 1162431181843410335992166400120182095388286172995271560085552334547332017238980724901073295977757714912392919146582441932837
n01919133 11644431018193410335992166400120182095388286172995271560085552334547332017238980724901073295977757714912392919146582441932837
n02287777 1181481194172522834301390910612444169744442018732624574254368308355923028010039087026342541201361773134429661280
n03837318 11831142231481038268103877214841061388821098420364410982777661281342127041824582275318550933451789780751514881477
n00191248 11811721338103877214841061388821098420364410982777661281342127041824582275318550933451789780751514881477
n02810184 1174431103877214841061388821098420364410982777661281342127041824582275318550933451789780751514881477
n02280664 11800011248730103877214841061388821098420364410982777661281342127041824582275318550933451789780751514881477
n02142336 11811721338103877214841061388821098420364410982777661281342127041824582275318550933451789780751514881477
n02108657 11811721338103877214841061388821098420364410982777661281342127041824582275318550933451789780751514881477
n03709379 11811721338103877214841061388821098420364410982777661281342127041824582275318550933451789780751514881477
n0218533 11811721338103877214841061388821098420364410982777661281342127041824582275318550933451789780751514881477
n0117411 11811721338103877214841061388821098420364410982777661281342127041824582275318550933451789780751514881477
n028004 11811721338103877214841061388821098420364410982777661281342127041824582275318550933451789780751514881477
n0221014 11811721338103877214841061388821098420364410982777661281342127041824582275318550933451789780751514881477
n0223011 11811721338103877214841061388821098420364410982777661281342127041824582275318550933451789780751514881477
n02224131 11811721338103877214841061388821098420364410982777661281342127041824582275318550933451789780751514881477
n0210279 11811721338103877214841061388821098420364410982777661281342127041824582275318550933451789780751514881477
n0219824 11811721338103877214841061388821098420364410982777661281342127041824582275318550933451789780751514881477
n01983481 11811721338103877214841061388821098420364410982777661281342127041824582275318550933451789780751514881477

Visualization of the count per each of the 100 classes in the 'mask' version of ImageNet used by our approach.

482	256	484	56	320	82	436	42
48	40000	40000	40000	40000	40000	40000	40000
182	427	413	344	238	31	176	380
392	180	398	203	372	332	302	337
381	183	461	96	119	89	408	59
40	121	135	329	241	79	72	150
280	27	38	71	154	284	12	377
202	84	343	17	410	505	133	271
100	196	360	474	285	439	446	147
191	437	102	161	426	448	376	418
	449	68	405	114	445	36	479
		235	444	442	418	357	371

Visualization of the count per each of the 480 classes in the 'mask' version of OpenImages used by our approach. Class example, has 40k images.

Figure 2: Top half of the figure shows the count per class for the ImageNet dataset, the highest number of images in a given class is '1349' and the lowest count is '190'. The distribution in this case is not as skewed as the OpenImages (bottom half) dataset. About 60 classes in our subset of the OpenImages dataset account for half the dataset. The maximum and minimum counts are, 55K and 28 respectively.

as [1, 3]. We use the standard validation set along with ImageNet V2 [5] without any changes to the images.

In the case of OpenImages [4], we use the object detection dataset consisting of 600 classes and 1.7M images with 14M bounding boxes. However, the 600 classes also include many parent nodes and as this can contribute to label confusion. We remove all parent node classes and use only the leaf node classes. The dataset has bounding boxes for only a subset of images for commonly occurring objects and we remove these classes as well. Finally, we follow the approach of [?] and merge confusing classes. We end up with 480 classes and approximately 1.2M images. There are about 7 objects per image (average) in this subset and after applying the 'mask' method, we end up with approximately 6.8M images. Of these, about 1.3M images corresponded to the 'man' class and 'women' and 'windows' classes also had very high sample counts. We restrict the maximum number of images in a given class to around 50K and end up with roughly 2.2M images. We apply the same methodology to the val and test splits but we do not clip the sample counts per class.

Even after clipping the sample counts, the OpenImages dataset is very skewed compared to ImageNet as shown in figure 2, and we believe this imbalance makes OpenImages unsuitable for training good classifiers.

1.2 Hyperparameters

We use standard data-augmentation strategies like random cropping, scaling, color jitter, etc., for all methods and train all our ImageNet models for 300 epochs starting with a learning rate of 0.1 and decayed by 0.1 at epochs 75, 150, and 225 using a batch size of 256. For a fair comparison with our ImageNet-‘mask’ based models, we matched the number of iterations and reduced the total epochs for our OpenImages classifiers. We trained all our OpenImages models for 72 epochs starting with a learning rate of 0.1, and decayed by 0.1 at epochs 18, 36, and 54 using a batch size of 256. We assume that this reduced number of epochs also contributed to poor localization for the transfer learning case.

1.3 Hardware and software

All our experiments were run on ‘Dell C4130’ nodes, equipped with 4 Nvidia V100 cards each. We used Docker to maintain the same set of libraries across multiple nodes. The host environment was running ubuntu 18.04 with cuda 10.2 installed. The docker environment used ubuntu 16.04 with cuda 9.0 and PyTorch 1.1 and Anaconda python 4.3. We will release all our code and pretrained models before the conference.

1.4 Runtimes

Our *adaptive* label smoothing approach using the ‘mask’ version of ImageNet took approximately 74 hours and the hard label version took approximately 48 hours for 300 epochs. The object detection experiments took approximately 34 hours for 10 epochs.

2 Results

We provide more detailed results that were left out due to space constraints in the main paper.

2.1 Class activation maps

We provide more class activation maps to visualize the localization performance of baseline approaches, as well as our approaches in figures 3 and 4.

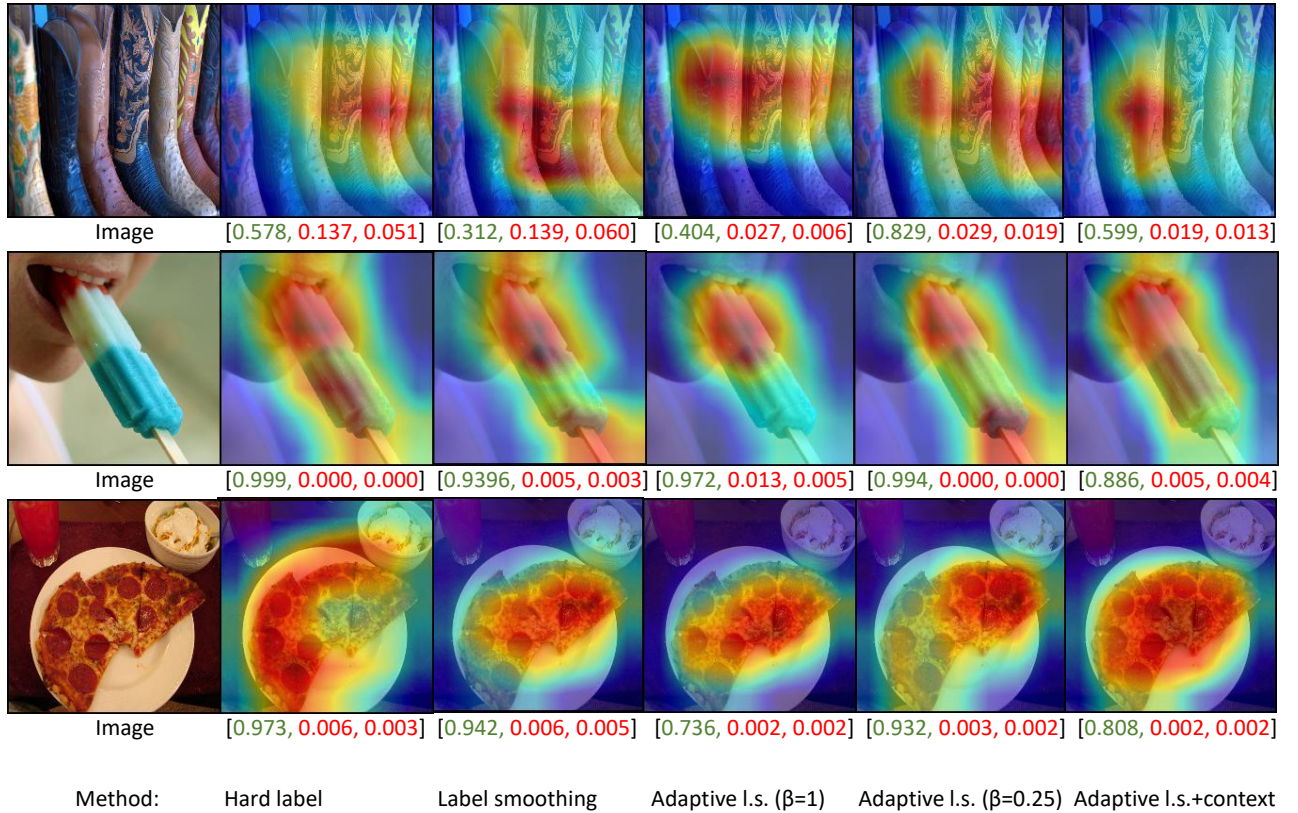


Figure 3: Examples of class activation maps (CAMs). These were obtained using the implementation of [2]. The second and third columns from the left show results for baseline CNNs using hard labels and standard label smoothing. Our approach, *adaptive* label smoothing (‘Adaptive l.s.’), is illustrated in the three rightmost columns. Our technique produces high-entropy predictions and shows an improved localization performance. The values under each CAM represent the top three probabilities, with green indicating the pertinent class and red indicating an incorrect prediction.

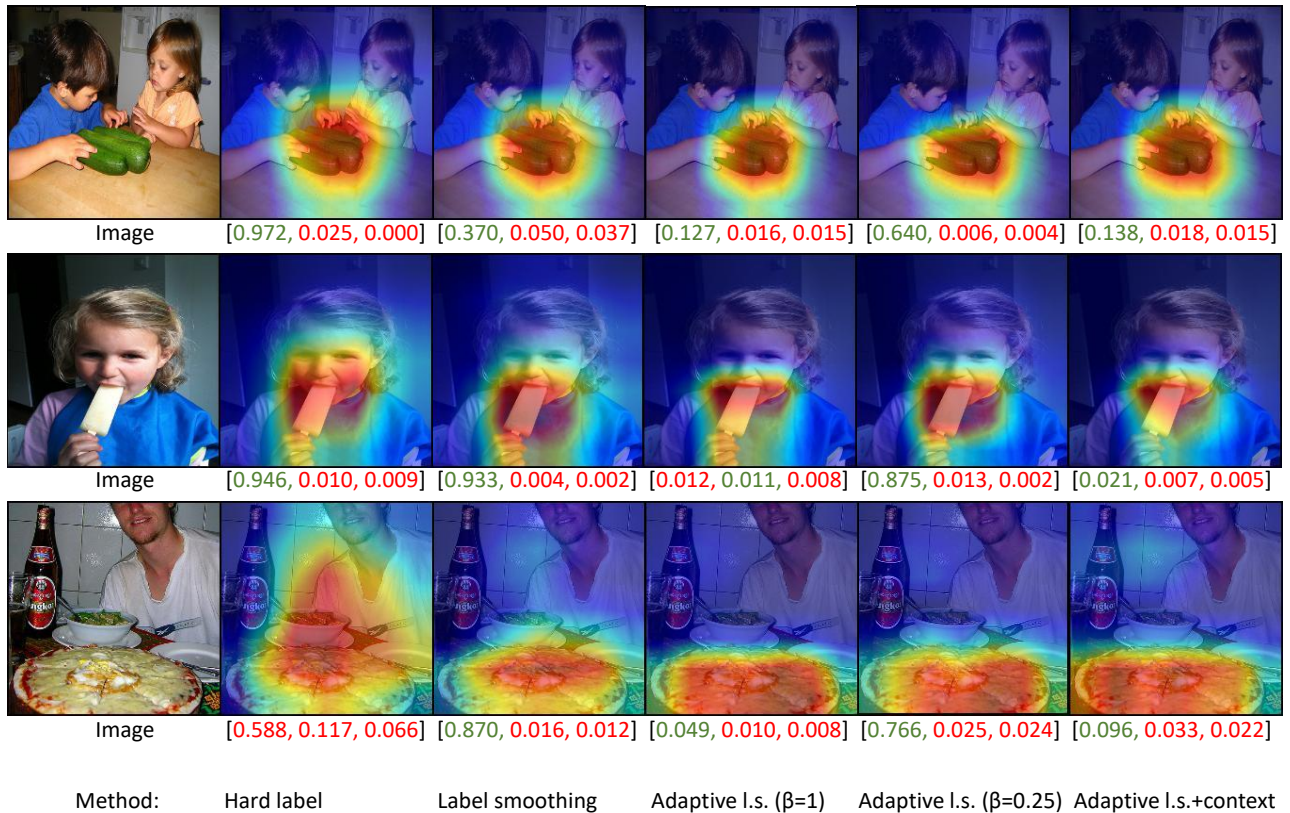


Figure 4: Examples of class activation maps (CAMs). These were obtained using the implementation of [2]. The second and third columns from the left show results for baseline CNNs using hard labels and standard label smoothing. Our approach, *adaptive* label smoothing (‘Adaptive l.s.’), is illustrated in the three rightmost columns. Our technique produces high-entropy predictions and shows an improved localization performance. The values under each CAM represent the top three probabilities, with green indicating the pertinent class and red indicating an incorrect prediction.

2.2 Tables

We provide detailed calibration metrics with mean and standard deviation for ImageNet and OpenImages classifiers in tables 1 and 2 respectively. We also provide AP (average precision) measures for different object sizes in table 3.

Table 1: Classification and calibration results with ImageNet. For a detailed explanation of the metrics please refer to section 4.2 in the main paper. ‘A.conf’, ‘O.conf’ and ‘U.conf’ refer to average confidence, overconfidence, and underconfidence scores. We provide ECE values for 100 bins and 15 bins mean scores along with their standard deviation (std).

Method	Val. Set	Train (N)	Acc. mean	Log-loss mean	ECE 100 mean	ECE 100 std	ECE 15 mean	ECE 15 std	MCE mean	MCE std	O.conf mean
Hard Label	V1	1.28M	0.769	0.963	0.062	0.003	0.045	0.003	0.284	0.069	0.582
Hard Label	V2	1.28M	0.647	1.643	0.131	0.006	0.099	0.006	0.664	0.166	0.538
CutMix	V1	1.28M	0.788	0.882	0.035	0.002	0.022	0.003	0.267	0.085	0.520
CutMix	V2	1.28M	0.661	1.499	0.094	0.007	0.051	0.005	0.817	0.183	0.485
RICAP	V1	1.28M	0.782	0.896	0.032	0.002	0.021	0.002	0.284	0.087	0.553
RICAP	V2	1.28M	0.663	1.533	0.108	0.010	0.072	0.013	0.697	0.168	0.516
Hard Label	V1	0.474M	0.669	1.568	0.104	0.005	0.093	0.005	0.347	0.068	0.558
Hard Label	V2	0.474M	0.543	2.365	0.171	0.014	0.148	0.012	0.759	0.162	0.520
CutMix	V1	0.474M	0.689	1.368	0.032	0.002	0.017	0.002	0.167	0.029	0.456
CutMix	V2	0.474M	0.577	2.021	0.100	0.008	0.050	0.008	0.517	0.169	0.421
Label Smoothing	V1	0.474M	0.691	1.428	0.055	0.002	0.051	0.002	0.354	0.241	0.401
Label Smoothing	V2	0.474M	0.558	2.107	0.102	0.006	0.047	0.010	0.512	0.111	0.368
A. L.S.	V1	0.474M	0.655	2.121	0.191	0.003	0.186	0.003	0.461	0.020	0.255
A. L.S.	V2	0.474M	0.532	2.839	0.185	0.011	0.158	0.012	0.661	0.071	0.217
Hard Label (mask)	V1	0.528M	0.680	1.451	0.088	0.003	0.076	0.004	0.259	0.025	0.549
Hard Label (mask)	V2	0.528M	0.559	2.194	0.155	0.007	0.127	0.011	0.686	0.106	0.507
CutMix (mask)	V1	0.528M	0.698	1.326	0.032	0.002	0.020	0.003	0.249	0.128	0.477
CutMix (mask)	V2	0.528M	0.576	1.999	0.110	0.008	0.067	0.008	0.614	0.100	0.449
Label Smoothing (mask)	V1	0.528M	0.687	1.447	0.051	0.002	0.046	0.003	0.430	0.311	0.407
Label Smoothing (mask)	V2	0.528M	0.563	2.135	0.108	0.005	0.048	0.007	0.524	0.074	0.374
A. L.S. (mask)	V1	0.528M	0.648	2.176	0.186	0.002	0.182	0.002	0.463	0.038	0.246
A. L.S. (mask)	V2	0.528M	0.528	2.914	0.185	0.005	0.160	0.006	0.687	0.074	0.209
A. L.S. (mask) (beta =0.75)	V1	0.528M	0.681	1.759	0.146	0.004	0.142	0.003	0.377	0.020	0.319
A. L.S. (mask) (beta =0.75)	V2	0.528M	0.556	2.478	0.146	0.009	0.113	0.013	0.572	0.119	0.274
A. L.S. (mask) (beta =0.25)	V1	0.528M	0.684	1.479	0.059	0.003	0.052	0.004	0.244	0.025	0.402
A. L.S. (mask) (beta =0.25)	V2	0.528M	0.561	2.191	0.109	0.009	0.059	0.009	0.627	0.264	0.369
A. L.S. + Context (mask)	V1	0.528M	0.637	2.197	0.174	0.004	0.169	0.004	0.431	0.023	0.251
A. L.S. + Context (mask)	V2	0.528M	0.515	2.954	0.177	0.009	0.147	0.007	0.682	0.069	0.221
A. L.S. + CutMix (mask)	V1	0.528M	0.442	4.569	0.349	0.004	0.332	0.004	0.559	0.029	0.047
A. L.S. + CutMix (mask)	V2	0.528M	0.346	4.952	0.292	0.011	0.265	0.012	0.902	0.070	0.049

Table 2: Classification and calibration results with OpenImages. For a detailed explanation of the metrics please refer to section 4.2 in the main paper. ‘A.conf’, ‘O.conf’ and ‘U.conf’ refer to average confidence, overconfidence, and underconfidence scores. We provide ECE values for 100 bins and 15 bins mean scores along with their standard deviation (std).

Method	Val./Test size	Val. Set	Acc. mean	Log-loss mean	ECE 100 mean	ECE 100 std	ECE 15 mean	ECE 15 std	MCE mean	MCE std	O.conf mean
Hard Label (mask)	105978	Val	0.552	1.519	0.089	0.003	0.080	0.004	0.280	0.029	0.476
Hard Label (mask)	325098	Test	0.549	1.522	0.089	0.002	0.083	0.002	0.262	0.073	0.479
Label Smoothing (mask)	105978	Val	0.554	1.573	0.044	0.003	0.032	0.004	0.220	0.061	0.410
Label Smoothing (mask)	325098	Test	0.550	1.577	0.033	0.002	0.029	0.002	0.196	0.148	0.408
A. L.S. (mask)	105978	Val	0.392	4.725	0.389	0.008	0.372	0.008	0.779	0.117	0.032
A. L.S. (mask)	325098	Test	0.388	4.749	0.346	0.004	0.328	0.004	0.579	0.018	0.031
A. L.S. (mask) + Context	105978	Val	0.383	4.049	0.219	0.005	0.203	0.005	0.464	0.028	0.092
A. L.S. (mask) + Context	325098	Test	0.371	4.092	0.193	0.003	0.178	0.002	0.415	0.022	0.089
A. L.S. (mask) (beta =0.25)	105978	Val	0.556	1.667	0.058	0.003	0.051	0.003	0.226	0.094	0.371
A. L.S. (mask) (beta =0.25)	325098	Test	0.554	1.670	0.052	0.002	0.049	0.002	0.127	0.010	0.370

Table 3: Fine-tuning on COCO using FRCNN for object detection. For a detailed explanation of the results please refer to section 4.3 in the main paper. AP refers to average precision and AR refers to average recall at the specified Intersection over union (IoU) level. We also provide AP values for small, medium, and large objects using ‘S’, ‘M’, and ‘L’ respectively.

Method	Pre-train dataset	Pre-train size	AP 0.5:0.95	AP 0.5	AP 0.75	AP (S) 0.5:0.95	AP (M) 0.5:0.95	AP (L) 0.5:0.95
Hard Label	ImageNet	1.28M	0.323	0.519	0.345	0.136	0.367	0.481
CutMix	ImageNet	1.28M	0.329	0.528	0.353	0.139	0.376	0.490
RICAP	ImageNet	1.28M	0.331	0.528	0.354	0.138	0.376	0.493
Hard Label	ImageNet	0.474M	0.290	0.479	0.309	0.112	0.325	0.437
Adaptive L.S.	ImageNet	0.474M	0.311	0.501	0.332	0.119	0.352	0.470
Hard Label (mask)	ImageNet	0.528M	0.290	0.482	0.307	0.114	0.329	0.435
CutMix (mask)	ImageNet	0.528M	0.312	0.509	0.329	0.125	0.353	0.470
Label Smoothing (mask)	ImageNet	0.528M	0.304	0.500	0.324	0.122	0.346	0.455
Adaptive L.S. (mask)	ImageNet	0.528M	0.311	0.501	0.333	0.124	0.351	0.477
Adaptive L.S. (mask) (beta =0.75)	ImageNet	0.528M	0.309	0.498	0.331	0.123	0.348	0.467
Adaptive L.S. (mask) (beta =0.25)	ImageNet	0.528M	0.298	0.492	0.315	0.122	0.340	0.449
Adaptive L.S. + Context (mask)	ImageNet	0.528M	0.303	0.490	0.323	0.115	0.339	0.465
Adaptive L.S. + CutMix (mask)	ImageNet	0.528M	0.273	0.449	0.289	0.098	0.300	0.423
Hard Label (mask)	OpenImages	1.20M	0.295	0.484	0.313	0.115	0.330	0.453
Label Smoothing (mask)	OpenImages	1.20M	0.301	0.493	0.320	0.119	0.339	0.457
Adaptive L.S. (mask)	OpenImages	1.20M	0.243	0.415	0.250	0.083	0.263	0.376
Adaptive L.S. + Context (mask)	OpenImages	1.20M	0.289	0.471	0.308	0.111	0.321	0.448
Adaptive L.S. (mask) (beta =0.25)	OpenImages	1.20M	0.304	0.494	0.324	0.118	0.340	0.462

3 Future work

This paper has addressed the problems of contextual bias and calibration using a novel approach called *adaptive* label smoothing. We hope weakly supervised localization methods can be used to provide object proportion information for large classification datasets and our approach can be applied to them to obtain further gains in performance. We are currently extending this work to out of distribution detection as well.

References

- [1] Lisa Anne Hendricks, Kaylee Burns, Kate Saenko, Trevor Darrell, and Anna Rohrbach. Women also snowboard: Overcoming bias in captioning models. In *Proceedings of the European Conference on Computer Vision (ECCV)*, pages 771–787, 2018.
- [2] Aditya Chattopadhyay, Anirban Sarkar, Prantik Howlader, and Vineeth N Balasubramanian. Grad-cam++: Generalized gradient-based visual explanations for deep convolutional networks. In *2018 IEEE Winter Conference on Applications of Computer Vision (WACV)*, pages 839–847. IEEE, 2018.
- [3] Jinwoo Choi, Chen Gao, Joseph CE Messou, and Jia-Bin Huang. Why can't i dance in the mall? learning to mitigate scene bias in action recognition. In *Advances in Neural Information Processing Systems*, pages 851–863, 2019.
- [4] Alina Kuznetsova, Hassan Rom, Neil Alldrin, Jasper Uijlings, Ivan Krasin, Jordi Pont-Tuset, Shahab Kamali, Stefan Popov, Matteo Mallocci, Alexander Kolesnikov, et al. The open images dataset v4. *International Journal of Computer Vision*, pages 1–26, 2020.
- [5] Benjamin Recht, Rebecca Roelofs, Ludwig Schmidt, and Vaishal Shankar. Do imagenet classifiers generalize to imagenet? In *International Conference on Machine Learning*, pages 5389–5400, 2019.
- [6] Olga Russakovsky, Jia Deng, Hao Su, Jonathan Krause, Sanjeev Satheesh, Sean Ma, Zhiheng Huang, Andrej Karpathy, Aditya Khosla, Michael Bernstein, Alexander C. Berg, and Li Fei-Fei. Imagenet large scale visual recognition challenge. *International Journal of Computer Vision*, 115(3):211–252, 2015.